Computational Geosciences (2006) 10:61–96
DOI: 10.1007/s10596-005-9011-5 © Springer 2006

Real-time reservoir management: A multiscale adaptive optimization and control approach

L. Saputelli[a,b], M. Nikolaou[b] and M. J. Economides[b]

[a]*Landmark Division, Halliburton, 2101 City West Blvd., Houston, TX 77042, USA*
E-mail: luigi.saputelli@halliburton.com
[b]*Chemical Engineering Department, University of Houston, Houston, TX 77204-4004, USA*

Accepted 8 August 2005

We propose a decision-making approach for optimizing the profitability of hydrocarbon reservoirs. The proposed approach addresses the overwhelming complexity of the overall optimization problem by suggesting an oilfield operations hierarchy that entails different time scales. We discuss system identification, optimization, and control that are appropriate at various levels of the hierarchy and capitalize on the abilities of permanently instrumented and remotely actuated fields. Optimization is performed in real-time and is based on feedback. We provide details on real-time identification of hybrid models and their use at the scheduling and supervisory control levels. Case studies using field-calibrated simulation data demonstrate the applicability and value of the proposed approach. Directions for future development are given.

Keywords: real-time, system identification, model predictive control, advanced process control, reservoir management, production optimization, smart fields, intelligent wells

1. Introduction

1.1. Modeling for reservoir management

The widely cited end of "easy oil era" is creating unprecedented challenges for hydrocarbon reservoir management. To successfully address such challenges, the oil and gas industry is relying on a number of factors, one of which is new technologies. Frequently referred to as "smart" or "intelligent", among others [1], such technologies offer exciting new capabilities for remote sensing (e.g., wellbore sensors, 4D seismic) and actuation (e.g., internal control valves) of wells. The main value of remote sensing and actuation is that they are critical enabling components in feedback-based decision-making loops (whether manual or automatic), where (a) data are continually collected,

(b) decisions are made, and (c) actions are taken. However, the full value of sensing and actuation cannot be realized unless they are integrated with appropriate decision-making methods. An important aid to decision making is mathematical modeling, namely, the capability to predict, explicitly or implicitly, the future outcome of deliberate actions, so that the "best" actions can be decided upon. This, in turn, creates the problem of (a) what kind of models to use, (b) what criteria to use to make decisions, and (c) how. Addressing this problem in its entirety is beyond reach. Rather, a meaningful decomposition of the problem is warranted. In that respect, a multilevel decomposition of the field-wide optimization problem is shown in figure 1 [22]. The proposed framework has the following key features:

- It casts field-wide optimization–a problem of unmanageable complexity–as multilevel optimization. Levels are separated according to time scale. At each level, decisions are made at the pertinent time scale.
- It emphasizes real-time optimization, where the term "real-time" refers to making decisions at a frequency commensurate with the time-scale of the corresponding level.
- It obviates the need to consider a variety of modeling and optimization paradigms, depending on the pertinent level.
- It integrates field data for continuous learning of key features of the managed system, based on a variety of models suitable for real-time operations.

The main message of this paper is that such a multilevel decomposition naturally necessitates various modeling (and corresponding decision making) paradigms, ranging, for example, from large-scale reservoir simulators used in sophisticated alrgorithmic optimization to simple empirical models for fluid flow. Modeling paradigms can be based on first principles, empiricism, or a combination thereof. The choice of the appropriate paradigm is dictated by both technical and economic criteria. In fact, the additional cost and infrastructure complexity that "smart" or "intelligent" solutions usually impart should be offset by increased value. When properly selected and implemented, smart technologies have added value in many occasions ([2] and references therein) and may be the only solution for well-identified candidates such as deep offshore and remote developments.

1.2. Contents of this work

To demonstrate the capabilities of the proposed approach, we present a case study concerning the interplay between the decision-making levels referred to as scheduling, supervisory control/model predictive control (MPC), and regulatory control in figure 1. At the supervisory control/MPC level, we implement a model predictive (receding horizon) control scheme that underlies a scheduling optimization level, which, in turn, suggests the best operating points (production flow rates) of a

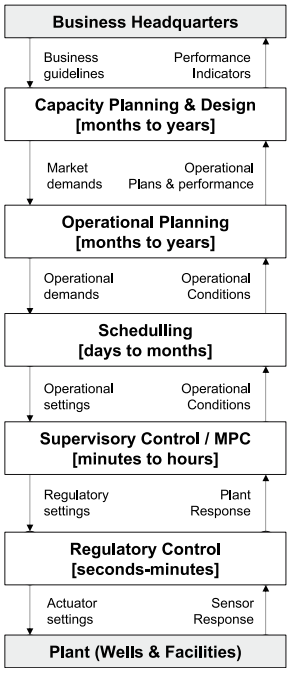

Figure 1. Field operations hierarchy after Saputelli et al. [22]. Arrows pointing down refer to decisions passed from upper levels to underlying levels, whereas arrows pointing up refer to information passed from underlying levels to upper levels. Note that feedback is essential for operations at all levels. Feedback-based decisions are made at different time scales, using a variety of decision-making tools corresponding to various modeling and optimization paradigms.

hydrocarbon producing field, as shown in figure 2, discussed in the sequel. The model used at the MPC level is semiempirical, while the model employed at the scheduling level is purely data-driven. For this study, we develop a software prototype, and test it by using a commercial reservoir and well modeling environment as a virtual field. Dynamic simulations show that the proposed strategy results in significant reduction of water injected and produced, with simultaneous increase in overall oil recovery. The self-learning reservoir management strategy is able to reduce cumulative water production by almost 80% and reduce water injection by 55%, thus increasing project profitability from 13% to 55%.

In the remainder of the paper, we first provide a critical presentation of background material related to current practice in reservoir planning and control as well as related experience of multilevel decision making in other industries. Next, we discuss data and model identification in real time. Subsequently, we describe how the simulation case study fits in the multilevel framework of figure 1, and present the case study. Finally, we draw conclusions and offer recommendations for future work.

2. Background on reservoir production planning and control

2.1. Current practices, challenges, and opportunities

In standard practice, engineers use a numerical reservoir model to simulate multiple future production scenarios, and select the best one either heuristically or by solving a related optimization problem. However, the selected scenario is hardly ever followed in practice, due to various inevitable practical difficulties (e.g., budget uncertainties, project delays, availability of resources, unforeseen disturbances and upsets). As a result, what was the forecasted optimal production scenario at the time when optimization was performed may actually be irrelevant to the actual production conditions as production progresses (e.g., fewer wells drilled than planned, wells completed in a different target zone, water injection rates off target). Consequently, the modeling and optimization exercise must be repeated as new conditions and production data become available [3]. But updating the reservoir model used by a numerical simulator through history matching (adjustment of model parameters to match production history) is a laborious task whose frequent repetition is often unwieldy from a practical viewpoint. In fact, history matching may easily take a year or two, during which time additional discrepancies are certain to arise between the data used to update the model and actual production.

Because of the above, output from the numerical reservoir simulator is not suitable for accurate short-term predictions that are necessary for optimization of daily production. To address this, people have used alternative methods such as decline curve analysis–which is not suitable for optimization [4]–and inflow performance relationships [5]–without frequent update. Therefore, there would be significant value in a mathematical modeling approach, which can make reliable short-term predictions that are crucial for production-related optimal decision making.

Making use of the increased availability of real-time data in the field, many pertinent propositions have also appeared that address data-driven decision making for production-related issues using various tools, such as neural networks [6], Kalman filtering [7], wavelets [8], system identification, and principal component analysis [9]. A good collection of related examples is presented by Saputelli et al. [22].

While individually important, such propositions must also be viewed in the context of decision making for optimization of an entire oilfield operation, rather than individual aspects of it, if industrial impact is to be maximized. Therefore, articulating a framework that would facilitate the development and use of tools for (oil)field-wide optimal decision making would both increase the value of existing tools and stimulate the development of new ones.

2.2. Related experience

Multilevel decision making has been developed and extensively tested in the petrochemical industry over the last few decades [10]. The need for separation of tasks

according to time scale was realized early by practitioners in the field. Today, technology is available that addresses issues at all levels of figure 1 for the petrochemical industry. Even though challenges for further development remain, there is a good foundation on which to build. This foundation can prove extremely useful for related development in the oil industry. At the same time, it should be stressed that significant differences exist between an oil refinery or petrochemical plant and an oilfield. Therefore, efforts should be undertaken in earnest to identify both technologies that are suitable for use and promising areas for development and implementation of new technologies.

Despite having been extensively used in the petrochemical industry, multivariable optimization has not penetrated the oil industry to the same extent. To the extent that it is used, it lacks good real-time connection with the oilfield, and does not consider the inclusion of data for continuous updating of models. Nevertheless, multivariable optimization techniques have been used in many fragmented ways in the oil and gas industry to support decisions related to tasks such as resource scheduling [11], field development under uncertainty [12], automated history matching of reservoir parameters [13], optimal well location and spacing [14], production parameter settings [15–19], and optimization of the displacement efficiency or recovery factor [20]. Such optimization uses models that are generated off-line, either by using first principles, or semiempirically, by using data acquired in the field.

3. Real-time system identification

The mathematical model of a system can be based on first principles (e.g., conservation of momentum, mass, and energy), empiricism, or combination thereof. First-principles models can be combined with constitutive equations (e.g., Darcy's law, ideal gas law, pressure-drop relationships) to generate model structures that are valid over a wide range of operating conditions. However, such models may be cumbersome to develop and manipulate. Empirical models, on the other hand, may be easy to develop, provided sufficient data are available, but may not be as accurate and cannot be easily used outside the range of data used to fit the model parameters. Hybrid models may employ a first-principles structure along with empirical constitutive equations and rely on data to identify values of model parameters. Because of this, hybrid models are often easier to develop and manipulate than raw first-principle models, while maintaining model fidelity outside the range of the data used for model parameter identification.

3.1. Hybrid models and system identification

System identification refers to the process of building mathematical models of *systems* based on measured data [21]. The process by which one continuously uses

data to identify values of the parameters of an empirical or hybrid model is often referred to as *learning*. We call *self-learning* the process by which a system uses its own past operating data to build a related model.

At this point, it should be mentioned that the term *learning* has been extensively used in conjunction with neural networks to denote their ability to "learn arbitrarily complex non-linear mappings from available data." Even though the range of mappings that neural networks can approximate is extremely wide, learning is not a capability unique to neural networks, but one that is possessed by every parametric model structure, including standard linear model structures [22].

When data are scant, as is often the case in practice, one has to balance the accuracy of data fitting with the model's predictive ability, via appropriate selection of a model structure. In addition to model structure suggestions by first principles, various quantitative statistical criteria can also be used to that end (e.g., cross-validation [23], Akaike information criterion [24]).

For the above reasons, we propose to use hybrid models for self-learning reservoir management. Our aim is to reduce the brittleness of purely empirical (black-box) parametric models (such as neural networks) when extrapolating beyond the training data by forcing conformance to physical laws.

3.2. Parametric reservoir model

The first step toward developing a model is to state what the model will be used for. Models to be used for decision making must have explicitly designated sets of inputs and outputs. In addition, the predictive ability of such models should be evaluated based on how well they allow the optimum decision to be arrived at, rather than on the basis of overall prediction quality.

Consider the water drive production system shown in figure 2, which depicts an injector–producer configuration in a single-layer reservoir. Inputs to this model are the well flowing pressures p_{wf1} and p_{wf2}, which are manipulated by adjustment of corresponding choke valves on the injector and producer. Outputs of this model are the reservoir pressure P; the oil, water, and gas production rates, q_o, q_w, q_g; the water cut (percentage of water in the liquid production stream) f_w; and water injection rate, q_{wi}. Note that even though water injection corresponds to an inlet flow of the physical

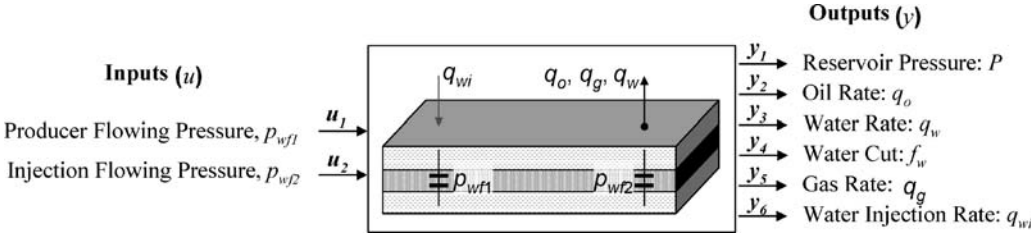

Figure 2. Waterflood in a single-layer reservoir with one water injection well and one production well.

system, the water injection rate as a signal is an output of the system, i.e., its value is determined by both the input signals to the system and the system itself, as shown in figure 2.

The well flow rates can be predicted by use of first-principles equations as described in Appendix A. Continuously acquired field data can be used to model the reservoir through relationships such as,

$$\begin{bmatrix} q_o^k & q_w^k & q_g^k & q_{wi}^k \end{bmatrix} = \begin{bmatrix} 1 & \overline{p}^k & p_{wf1}^k & \left(p_{wf1}^k\right)^2 & p_{wf2}^k & \left(p_{wf2}^k\right)^2 \end{bmatrix} \begin{bmatrix} a_0 & b_0 & c_0 & d_0 \\ a_1 & b_1 & c_1 & d_1 \\ a_2 & b_2 & c_2 & d_2 \\ a_3 & b_3 & c_3 & d_3 \\ a_4 & b_4 & c_3 & d_4 \\ a_5 & b_5 & c_5 & d_5 \end{bmatrix}, \quad (1)$$

and

$$\left[(\overline{p})^k\right] = \begin{bmatrix} e_0 & e_1 & e_2 & e_3 & e_4 & e_5 \end{bmatrix} \left[1 \ \overline{p}^{k-1} \ q_o^{k-1} \ q_w^{k-1} \ q_g^{k-1} \ q_{wi}^{k-1}\right]^T, \quad (2)$$

where k refers to a time instant. The nomenclature and derivation of equations (1) and (2) describe modeling of fluid flow rates and reservoir pressure by using simple analytical equations in agreement with Vogel's and Fetkovich's empirical equations for the well flow and Havlena–Odeh for the pressure equation.

Note that the above model is purely input–output and does not make explicit use of the internal states of the system (i.e., pressure, saturations, etc.). While knowledge of such internal states is generally valuable, it is not necessary for the purposes of optimization performed in this study. This greatly simplifies both the identification and optimization exercises.

3.3. *Parametric model extensions for more complex geological models*

Because models (Vogel's, Fetkovich's and Havlena–Odeh) capture the main and simplified physics features (i.e., well flow rate is a parametric combination of current flowing pressure; pressure is a parametric combination of mass flow rates), they can be used in a number of field cases where the variables to be estimated are also parametric combinations of the measured variables. For example, consider now a reservoir with two layers (figure 6). Flow rates may also be calculated by using equations (1) and (2). Flow rates can be calculated individually for each layer or as the summation of fluid rates in both layers. Average pressures can be calculated as the gross-rock volume-averaged pressure from all layers, or individual average reservoir pressure for each individual layer.

The simplified average pressure response may differ from the actual one up to a constant value. This difference can be adaptively eliminated within few iterations of the regression process (see "Parameter vector estimation"). Therefore, the approximation is adequately absorbed by the identification coefficients.

For future applications (e.g., different number of layers, wells, heterogeneous distribution of rock properties), a new set of system identification equations may be easily derived based on the required response and measured variables, as long as the variables to be estimated are still parametric combinations of the available measured variables.

3.4. Time scale effect on modeling

Note that equation (1) is based on the assumption that (a) the dominant time constant, T_1, corresponding to the dynamic response of $[q_o^k \; q_w^k \; q_g^k \; q_{wi}^k]^T$ to $[p_{wf1}^k \; p_{wf2}^k]^T$ is much smaller than the dominant time constant, T_2, corresponding to the decline of the average reservoir pressure, $\overline{p}$, and (b) the sampling period T, from time instant k to $k + 1$, is much larger than T_1, but comparable to or smaller than T_2. Consequently, in this case, equation (1) involves no dynamics under the preceding assumptions. Equation (2) involves first-order dynamics. Obviously, if one used a sampling period much smaller than T, then equation (1) would have to involve dynamics, whereas if the sampling period were much larger than T, both equations (1) and (2) would involve no dynamics. This makes it clear that what model one uses directly depends on the time scale at which the model is used.

3.5. State-space representation and alternatives

Substitution of equation (1) into equation (2) can bring the system equations into the standard state-space form,

$$\begin{aligned} \mathbf{x}^k &= \mathbf{f}\left(\mathbf{x}^{k-1}, \mathbf{u}^{k-1}\right) \\ \mathbf{y}^k &= \mathbf{g}\left(\mathbf{x}^k, \mathbf{u}^k\right), \end{aligned} \tag{3}$$

where, $\mathbf{u}^k$ is the input vector $[p_{wf1}^k \, p_{wf2}^k]^T$ at time instant k, $\mathbf{y}^k$ is the output vector $[q_o^k \, q_w^k q_g^k q_{wi}^k]^T$ at time k, $\mathbf{x}^k$ is the state vector $(\overline{p}\,)^k$, which–in this case–is a scalar, and $\mathbf{f}$ and $\mathbf{g}$ refer to the right-hand sides of equations (1) and (2). State-space representation of a system is standard in system theory. There exists a large body of work, developed over the last several decades, that can be used to analyze, optimize, and control systems described by such equations [25]. In addition, alternative representations exist in the time domain or in transform domains (e.g., Laplace or z domains). A particular model structure that we are also going to use in this work is the finite-impulse-response (FIR) model structure, which produces the output of a linear model by convolution on its input as

$$y^k = \sum_{i=1}^{n} h_i u^{k-i}, \tag{4}$$

The previously described input–output models [equations (1) and (2)] are conveniently transformed into equivalent FIR models, which are used when required in the

context of multivariate model predictive control formulation (Appendix B) represented by the Supervisory control hierarchy of figure 1 and the block diagram of figure 5.

3.6. Parameter vector estimation

The right-hand side of equations (1) and (2) includes certain coefficients that are estimated by regression using field data. For estimation to be possible, the collected data must be informative enough, namely, they must correspond to sufficient excitation of the process by its inputs. Because all coefficients appear linearly in equations (1) and (2), standard linear regression can be used for their estimation. By calling, $\mathbf{y}$ the measured values, and $\mathbf{y}_c = \mathbf{X}\widehat{\theta}$ the values predicted by the model, the estimate of the coefficient matrix, $\widehat{\theta}$, can be calculated as

$$\widehat{\theta} = \left(\mathbf{X}^T\mathbf{X}\right)^{-1}\mathbf{X}^T\mathbf{y} = \arg\left[\min_{\theta}\|\mathbf{y} - \mathbf{X}\theta\|^2\right], \tag{5}$$

which can be easily performed by standard numerical software and implemented on basic control hardware, such as field controllers. In case the model coefficients appear nonlinearly, then nonlinear regression can be used for their estimation.

Models such as the ones represented by equations (1) and (2) will vary with time. Therefore, the predictive ability of such models must be continuously evaluated. If such models are inadequate, they must be updated when new data become available. The success of both the model evaluation and updating tasks depend on the actual data collected, which must be sufficiently informative, as discussed below.

3.7. Need for informative data

It is a standard fact of linear regression that the variance of parameter estimator $\widehat{\theta}$ in equation (5) is proportional to the matrix $(\mathbf{X}^T\mathbf{X})^{-1}$. Consequently, the matrix $(\mathbf{X}^T\mathbf{X})$ must be at the very least invertible and preferably "large," namely, its smallest eigenvalue must be much larger than zero. Because the matrix $\mathbf{X}^T\mathbf{X}$ contains experimental data, it provides a direct characterization of what data are informative. From a practical viewpoint, informative data refers to data that excite the process. This should not be a problem in the oilfield, as permanent perturbations constantly excite the system being identified. In the case that field-captured data may not be informative enough, a persistent excitation process should be implemented [26].

3.8. Systematic dimensionality reduction

In many instances, data may be collected for a large number of variables or excessively frequently, resulting in highly correlated measurements. For example, this can happen in situations involving redundant sensors, oversampling, multiple wells, or multiple reservoir layers. In such cases, further reduction of dimensionality is

accomplished in a systematic way by using well-known multivariate analysis techniques such as principal components analysis (PCA) [27] and partial least squares (PLS) [28].

3.9. Model capabilities and limitations

As already noted, equation (1) is based on an empirical constitutive equation, namely, Vogel's equation, and equation (2) is a combination of mass balances and constitutive equations connecting flow and pressure. Because of that, models represented by equations (1) and (2) combine well-tested empiricism–no pun intended–with basic physics of well response to waterflooding (figure 2). Therefore, similar equations can be used for multilayer reservoirs with multiple injectors and producers (figure 6). For example, flow rates in a multilayer reservoir could be individually calculated for each layer or as the summation of both layers' fluid rates, depending on the configuration of field sensors. Also, in a given reservoir compartment, one could calculate the averaged pressure $\overline{p}$ over all layers, or, depending on available flow data, the individual averaged pressure $\overline{p}_i$ at each layer.

To identify the parameters of the models in equations (1) and (2), it is clear that historical data that are informative enough must be available. For example, to identify the coefficients $b_0, \ldots, b_5$ in equation (1), nonzero water production $\{q_w^k\}$ must have been observed, i.e., water must have broken through the producer well.

Because the model of equations (1) and (2) is approximate, it would have to be adapted as production progresses.

3.10. Comparison with traditional reservoir simulation

The proposed approach trades rigor for simplicity. Numerical reservoir simulation (NRS) considers a large number of physical effects captured by partial differential equations developed from first-principles and constitutive equations; however, the process is fairly complicated and laborious. NRS models incorporating the flow physics more directly will be preferable in cases where the long-term nonlinear behavior is unknown, and when rigorous studies are required for reservoir uncertainty management, e.g., field development planning, infill drilling, etc. In case of an asset already in production, the proposed approach can easily make use of historical data to match a model to measurements in a more automatic manner, leading to continuous adaptation as more data become available.

4. Multilevel control and optimization

4.1. Control and optimization for reservoir management

Well fluid rate control has been related to optimization of fluid displacement in porous media [29,30].

With the onset of intelligent wells, there has been an increasing need for development of control applications that will actuate this hardware. There have been attempts to model downhole valves and segmented well architectures [16], and to create optimization control routines [14,31,32] that will automatically adjust valve settings to optimize well and field throughput [17–19].

Some advanced recovery processes and novel architectures have also been subject to control and optimization treatment. Queipo et al. [33] suggested a surrogate model for the optimization of steam-assisted gravity drainage (SAGD) processes.

4.2. *Multilevel decision making*

The model presented in the previous section (equations (1) and (2)) is a good example of separation of time scales at different levels of the field operations hierarchy shown in figure 1. To make it even more clear how time scales are separated between levels, we show in figure 3 the specific locations where elements of equations (1) and (2) would fit, namely, from the scheduling level downwards. It is clear that details at additional levels may be explored.

4.3. *Supervisory/model predictive control level*

Model predictive control (MPC) is a class of computer control algorithms that explicitly use a plant model for on-line prediction of future plant behavior and

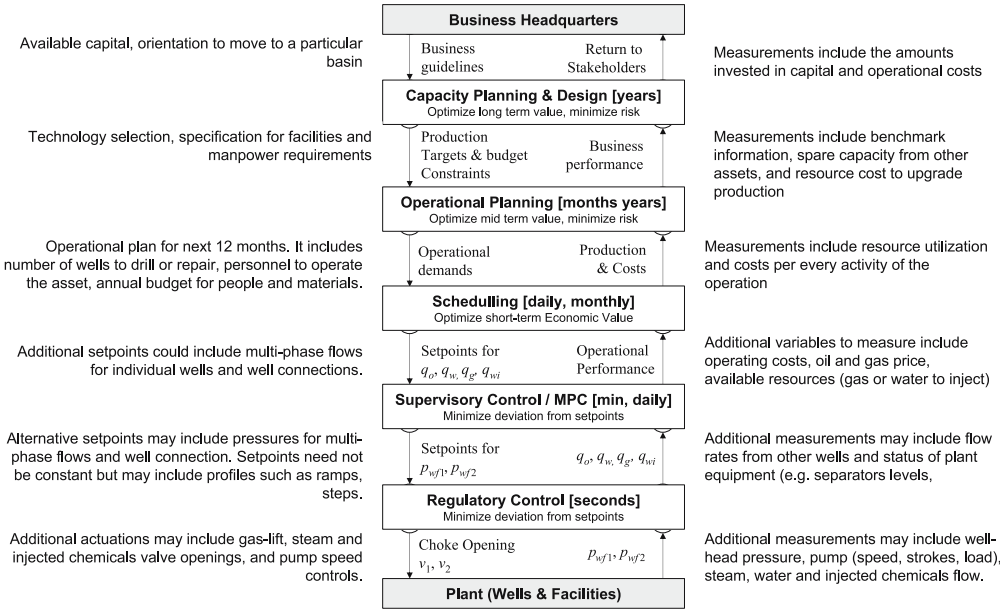

Figure 3. Field operations hierarchy for equations (1) and (2). Additional actuation and measurements are suggested for each level for more general cases.

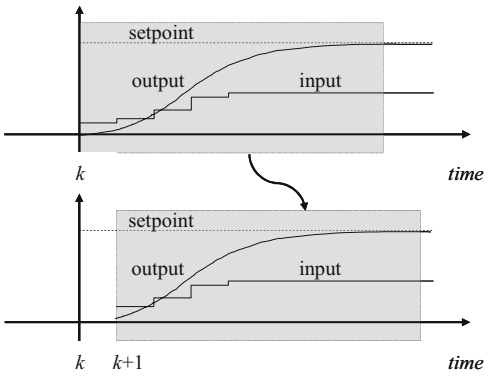

Figure 4. Moving horizon (shadow area) for model predictive control (MPC).

computation of appropriate control action through on-line optimization of a cost objective over a future horizon (figure 4), subject to various constraints [34,35]. Of the optimal input values calculated over the optimization horizon, the first value is implemented on the controlled process. The process is then left to operate until the next time point, when additional measurements are collected. The optimization horizon is subsequently shifted by one time point, and the on-line optimization problem is reformulated and solved. The entire procedure is repeated in the future.

Extensive experience in the downstream industry [10] as well as rigorous analysis [36,37] have proven the theoretical and practical value of MPC.

4.4. *Need for control-relevant models*

Because MPC explicitly uses a model in the on-line optimization, certain features of that model are critical for good feedback control performance. For example, consider a system satisfying the steady-state relationship $\mathbf{y} = \mathbf{G}\mathbf{u}$ between an input vector $\mathbf{u}$ and output vector $\mathbf{y}$, and assume that a model $\widetilde{\mathbf{G}}$ is built. For this system to be stabilizable by a feedback controller with integral action, the inequality $\mathrm{Re}[\lambda(\mathbf{G}\widetilde{\mathbf{G}}^{-1})] > 0$ must be satisfied [38]. It is not unusual (e.g., when a system is ill conditioned) for this inequality to be violated by models $\widetilde{\mathbf{G}}$, which would otherwise be considered very good approximations of $\mathbf{G}$.

4.5. *Comparison of optimal control and MPC*

A number of articles [20,29,30] have appeared about the use of optimal control for upstream problems. In comparison with optimal control, where the optimal profile of an input over a given horizon is calculated once, MPC solves an optimal control problem over the moving horizon not just once but repeatedly. Each time, the moving horizon has been shifted by one time point and new measurements are collected and

used to update the related optimization problem. Because of that, MPC is a feedback control strategy.

4.6. *Self-learning reservoir management (a two-level control and optimization)*

The following discussion shows that a self-learning reservoir management strategy can be achieved by combining the following three elements:

(a) Data-driven hybrid modeling,
(b) Supervisory/model predictive control,
(c) Scheduling optimization of the short-term net present value (NPV).

Figure 5 shows the structure resulting from interconnection of the above three elements. As shown in figure 5, the captured model at the Supervisory/MPC level (lower level) feeds a reservoir performance forecast block, which generates the fluid flow functions to be used in the NPV objective function. Optimization of the NPV objective function produces the setpoints that are fed to the MPC level (upper level).

4.7. *MPC Example*

Consider now the injector–producer problem in a two-layer reservoir (figure 6). Layers 1 and 2 are the producing units with distinctive (i.e., 10:1) permeability–thickness (*kh*) values, separated by an impermeable shale barrier. Inputs to this model are the well flowing pressures p_{wf1}, p_{wf2}, and p_{wf3}, which are manipulated by

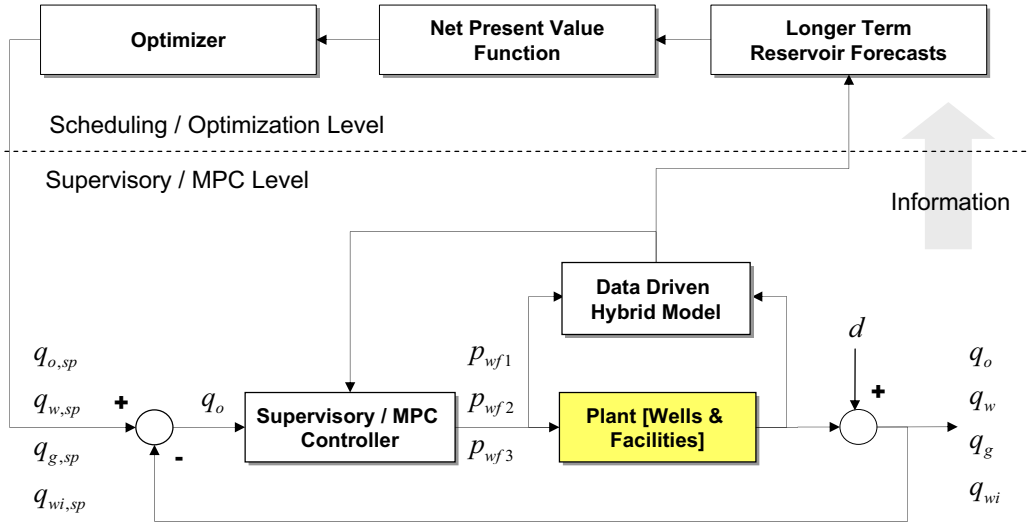

Figure 5. Bilevel self-learning reservoir control diagram.

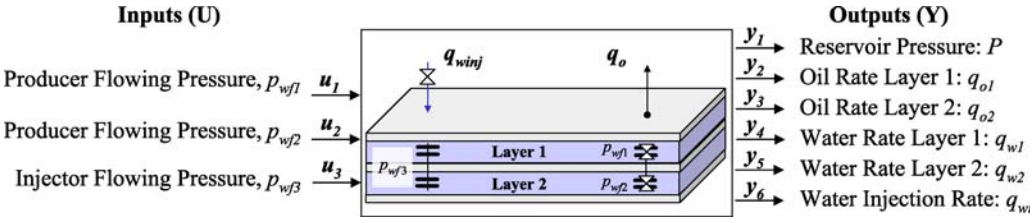

Figure 6. Waterflood injector–producer problem in multilayer reservoir. The producer has two independently controlled valves, whereas the injector has a single valve controlling total water injection.

adjustment of corresponding choke valves on the injector and producer. Outputs of this model are the reservoir pressure P; oil and water production rates, q_{o1}, q_{o2}, q_{w1}, and q_{w2} at the individual layers 1 and 2; and water injection rate, q_{wi}.

In Appendix B, we show the development of the basic elements of an MPC structure that includes simultaneous parametric identification of a reservoir model, as shown in figure 7. The structure of figure 7 includes an identification loop (upper part) and a feedback control loop (lower part). The identification loop identifies a model as structured input–output relationships similar to those of equations (1) and (2). This model is used by the lower part of figure 7, where an MPC controller implements process input for the next time step, based on the error between the setpoint and the actual process output. The objective function used for the MPC controller in closed loop (figure 7) is described by equation (B6).

Figure 8 shows an example of the structure of figure 7 in action, where the injector–producer problem of figure 6 is tested. The MPC parameter values in table 1 are used.

In the upper-left plot of figure 8, the setpoint of the average reservoir pressure is 10,000 psia and is kept within some constraints by the "aggressive" manipulation of the injector input (middle right of figure 8).

The setpoint for oil production (upper middle of figure 8) from each layer is changed to about 5,000 STB/D at t = 80 days. Bottomhole pressure (lower-left of

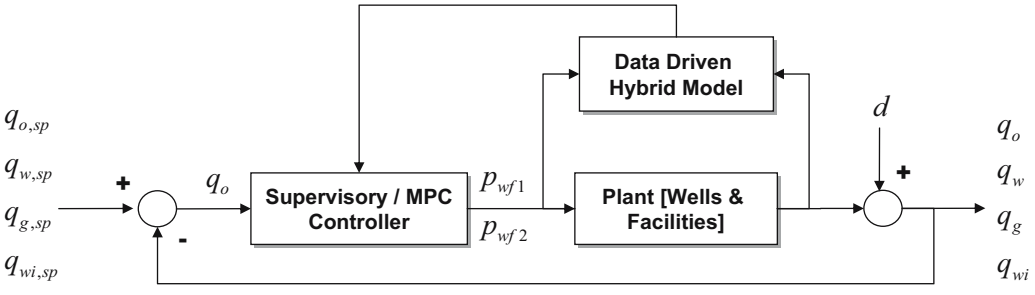

Figure 7. Model predictive control level and simultaneous identification implementation diagram.

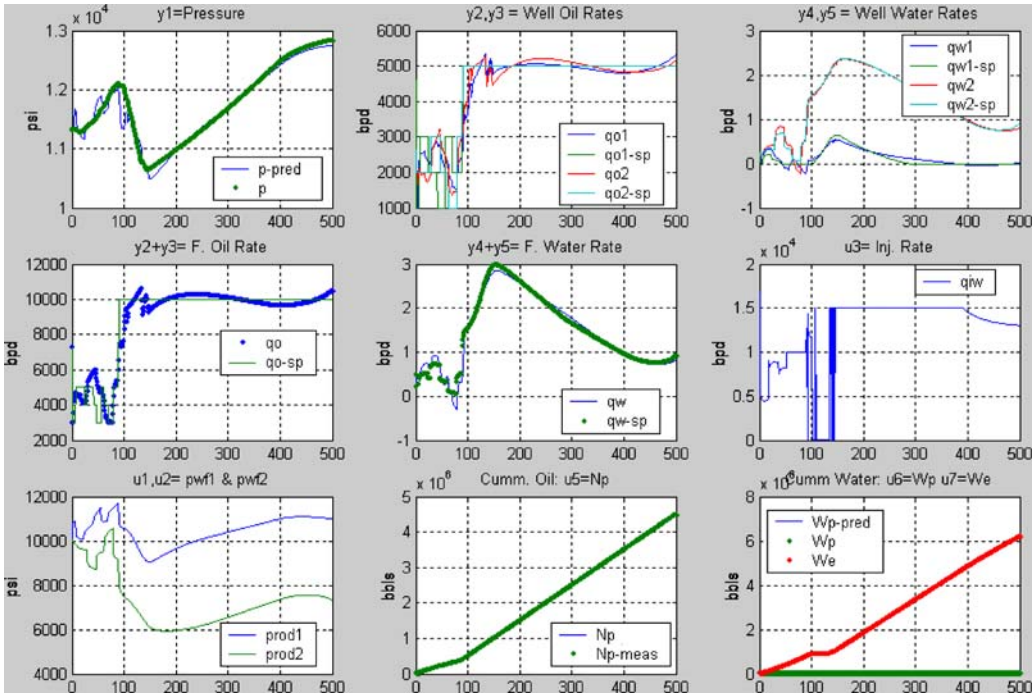

Figure 8. MPC injector–producer problem.

Table 1
MPC parameters values (for example, in figure 7)

Identification and prediction parameters	Input constraints	Output constraints
Days for identification = 30 days	$6{,}000 < p_{wf1} < P$	$10{,}000 < P < 13{,}000$
Prediction (moving) horizon = 10 days	$6{,}000 < p_{wf2} < P$	$0 < q_{o1} + q_{o2} + q_{w1} + q_{w2} < 12{,}000$
Simulation time = 500 days	$0 < p_{wf3} < 12{,}500$	$0 < q_{wi} < 15{,}000$

figure 8) in both layers is continuously adjusted to meet the setpoints. Because layer 1 has better reservoir properties, i.e., larger *kh*, the behavior of the bottomhole pressure is always above the one for layer 2, in order to meet the same target.

The change in oil production setpoint (at $t = 80$ days) is captured as a disturbance in the injector; after a short period, the injector is back on injection, and saturates its input to 15,000 BPD (barrels per day). After 150 days, reservoir pressure increases toward the upper limit.

4.8. *Scheduling level*

In the context of the field operations hierarchy (figures 1 and 3), a *scheduling level* is implemented (figure 5) to optimize the short-term NPV objective function

subject to current reservoir model and physical constraints. The objective function used for the scheduling level in closed loop is described in Appendix D. The optimization exercise reduces to

$$\max\left\{\mathrm{NPV}^k\right\} = \max_{u_1^k, u_2^k, u_3^k}\left\{\sum_{k=1}^{N} a u_1^k + b u_2^k + c u_3^k + d\right\} \tag{6}$$

where u_1, u_2, u_3 are the decision variables corresponding to the bottomhole pressures (p_{wf1}, p_{wf2}) of reservoir layers 1 and 2 for the producer, and the pressure of the water injection well, p_{wf3}; and a, b, c, and d are the resulting coefficients after combining locally linearized versions of the models of equations (1) and (2) with equation (D1), as explained in Appendix D. In general, the time point k would correspond to a time scale larger than the time scale of the MPC level (figure 3). For simplicity, in this work we consider equal time scale for both the scheduling and MPC levels. The value of N was selected to correspond approximately to 1 month, which is three times the MPC horizon length (figure 4).

The constraints are imposed by the reservoir, wells, surface equipment, cost, and schedule. For example, in finding the solution for optimizing the deliverability of a well, the physical constraints are given by the reservoir productivity and the tubing performance, as shown in figure 17, where the shaded area denotes the polytope of feasible solutions.

A linear programming optimization routine was used to find the optimum solution of equation (6). The solution vector is the set of operating variables that optimizes reservoir performance and value. This set of operating variables is the setpoint ($q_{\mathrm{o,sp}}$, $q_{\mathrm{w,sp}}$, $q_{\mathrm{g,sp}}$, and $q_{\mathrm{wi,sp}}$) of the MPC level that underlies this optimization level.

The above optimization exercise is carried on with the information available at every time step, assuming that future reservoir behavior is described by the current model. In subsequent time steps, that model is going to be updated and the NPV will be continuously refined.

5. Case study

5.1. Data-driven reservoir performance prediction–example

In this section, we show an application of the methodology that we presented in the previous sections. All reservoir data were generated by computer simulations using the commercial reservoir simulator Eclipse™ [39]. The simulator was calibrated using field production data (explained in Appendix C). The decision-making variables (inputs) and controlled variables (outputs) of that system are shown in figure 6.

To test the identification procedure, identification algorithms were used to identify the relationships between inputs and outputs in the context of equations (1) and (2). The identification algorithm considers the last 30 days of history, and

produces a model used to make predictions for the next 30 days. The results are shown in figure 9. Thirty-day-ahead predictions are shown after day 60. A good agreement is observed at the average reservoir pressure ($y_i \equiv P$), which is depicted in the upper left chart of figure 9. Oil rate fitting and prediction can be seen in the upper middle of figure 9, for which an exponential decline curve (red line) is also shown for comparison. The water production rate is presented in the upper right of figure 9.

Although the model cannot predict the onset of water before water has broken through, it is progressively adapted to the new wellbore conditions, i.e., it is transformed to represent water increase. A minor deviation in the prediction of water production can be observed (upper right of figure 9 at t = 740 days). However, the trend is preserved. Prediction of sudden changes in water injection rate (middle right of figure 9) was less accurate; however, the main features were captured.

Figure 10 shows the evolution with time of the identified parameters. One could appreciate the variation of each coefficient along time, i.e., the adaptability of the model to "learn" the system's variations. However, this is an indication of the difficulty to predict future performance for large horizons.

Variations in parameter estimates over time should not be directly related to physical process; however, they could be justified by the continuous and simultaneous

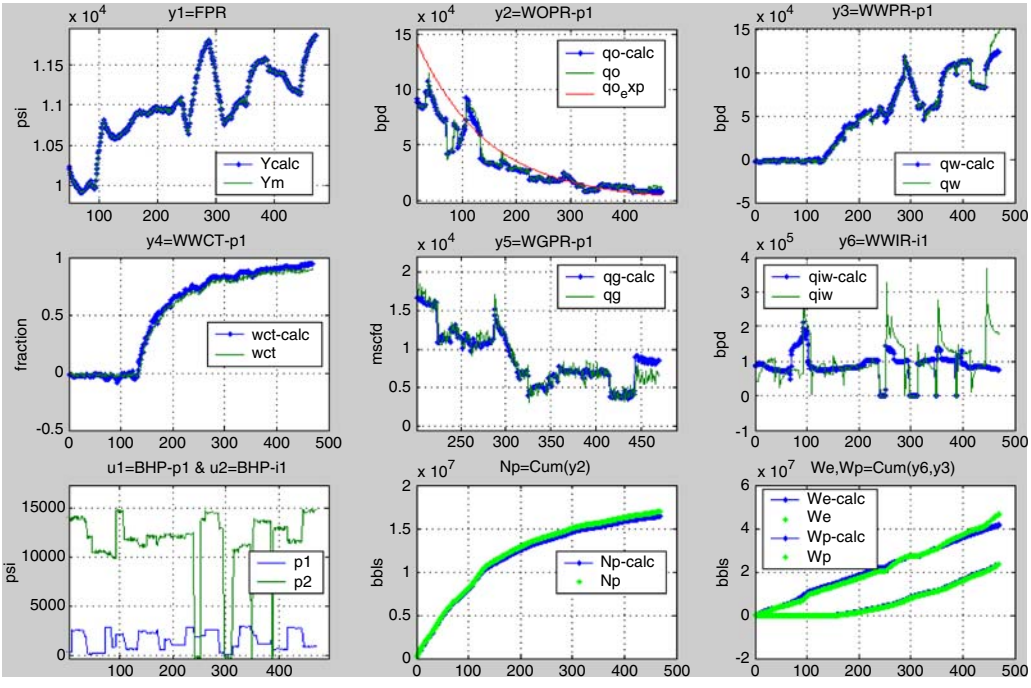

Figure 9. Reservoir performance prediction using parametric models.

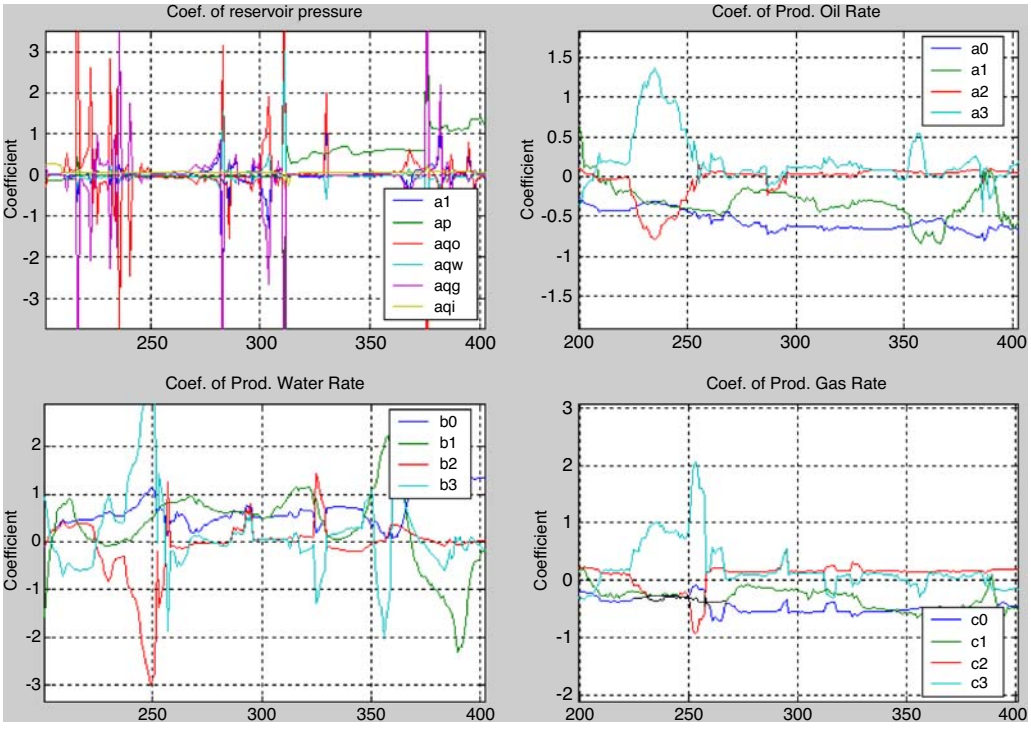

Figure 10. Parameter estimates as a function of time.

variations occurring near the reservoir, more profoundly near the wellbore, such as oil, water, and gas relative permeability, viscosity, and formation volume factors as a function of the changing pressure and phase saturations. Notice that in general the bias terms (a_0 and c_0) are well behaved and tend to have a constant value. One could also impose constraints in the way these parameters are allowed to change. This could bring even more stability to the model prediction performance.

5.2. *Closed-loop reservoir management example*

A five-spot waterflooding pattern is studied to understand the behavior of the closed-loop reservoir management strategy under the complexity of a field-wide production. A multilayer reservoir with five distinct *kh* values is used. Rock and fluid properties are described in Appendix C.

The five-spot waterflooding problem is exposed to both noncontrolled and multilevel controlled (self-learning reservoir management) strategies. Figures 11–14 show the simulation results under both strategies.

Figures 11 and 12 show the distribution of fluids (oil saturation) at the end of the simulation (2,200 days). The noncontrolled case (figure 11) showed early water

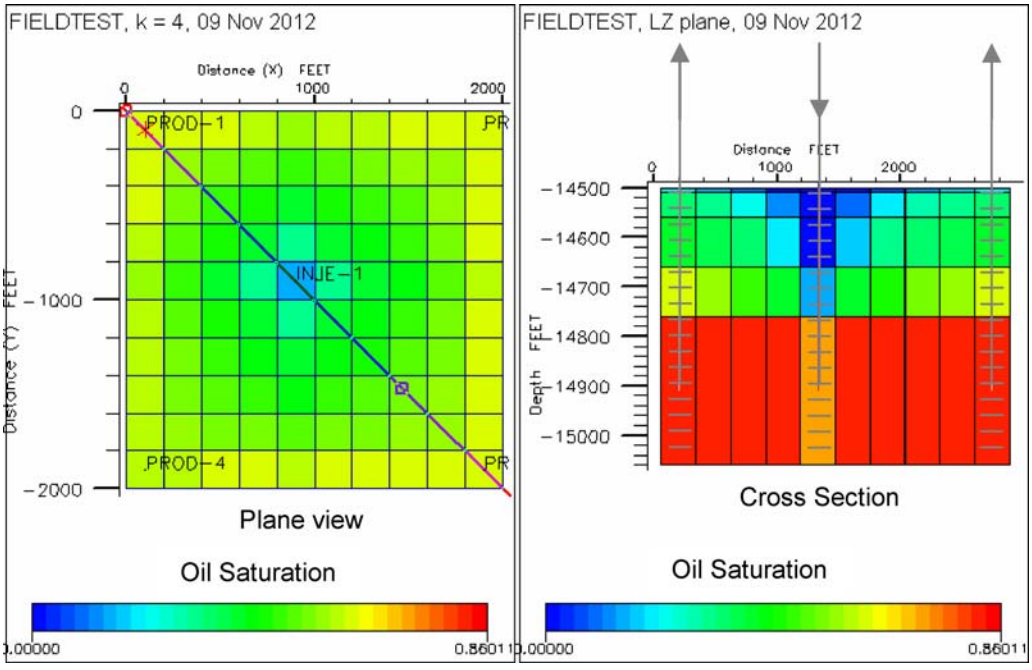

Figure 11. Five-spot water drive problem under no control management.

breakthrough in layer 1 (upper layer of high permeability), which reduced the ability of the well to flow under current vertical lift performance constraints. The ultimate recovery is impaired due to the inability of the well to lift high water cut flow rates.

The simulation under the self-learning reservoir management strategy (figure 12) shows a more uniform distribution than the one under no control (figure 11); water breakthrough was detected and controlled; bottomhole pressure inputs in the watered areas were reduced up to full zone shutoff. This permitted better vertical lift on the well. For the same period of time, recovery was accelerated at a minimum effort.

Although the vertical sweep efficiency looks better for the self-learning reservoir management case, both cross sections (figures 11 and 12) show similar fluid distribution, i.e., there are no dramatic differences.

However, it is noticeable that water breakthrough in layers 1 and 2 is delayed for the self-learning reservoir management case (figure 12). In the following graphs (figures 13 and 14), rates and cumulative fluids are compared for each case.

Oil rate and cumulative oil (figures 13 and 14) look slightly better for the self-learning reservoir management case, i.e., there is only a 5% increase in oil recovery, which is equivalent to an increase in net present value of about US$5 million over the project life.

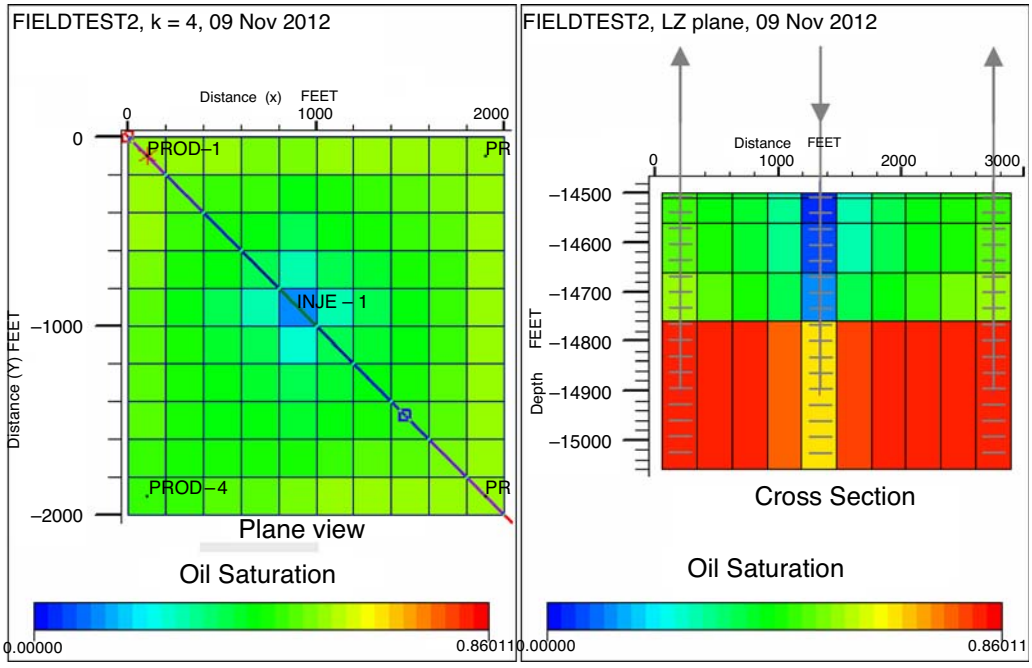

Figure 12. Self-learning reservoir management applied to five-spot water drive problem.

However, a more remarkable result is shown for the water produced and injected. As water breaks through (t = 50 days) in the high-permeability layers, it is detected and controlled in the self-learning mode (figure 6), where the simulation shows the continuous control and adaptation to better performance. As more water is produced

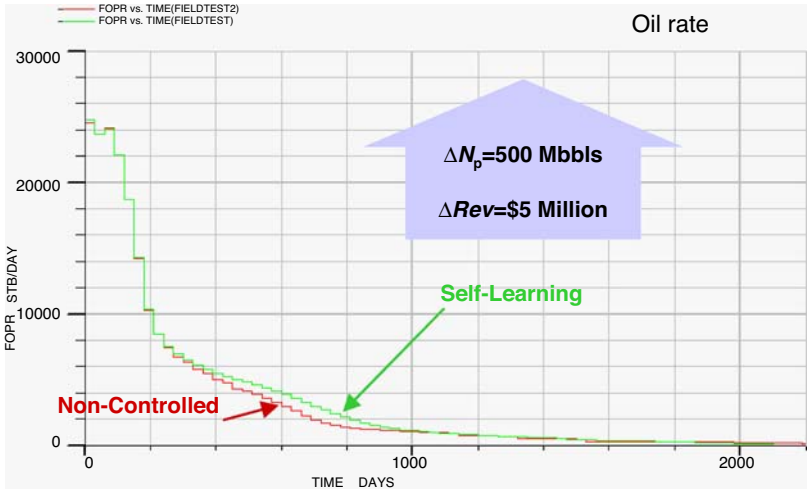

Figure 13. Oil rate comparison (five-spot water drive problem).

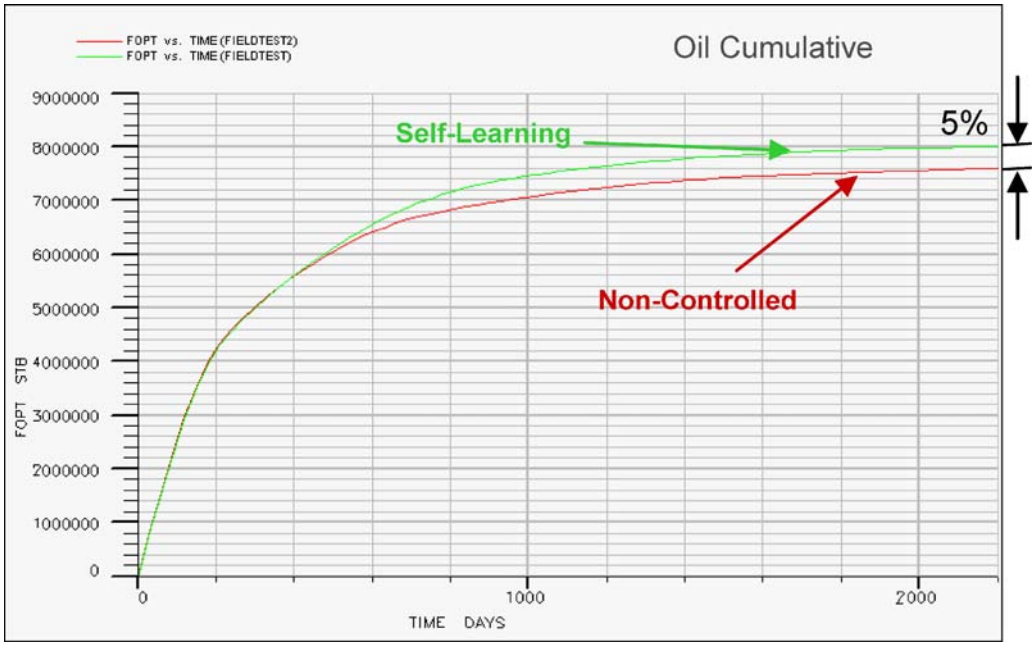

Figure 14. Oil cumulative comparison (five-spot water drive problem).

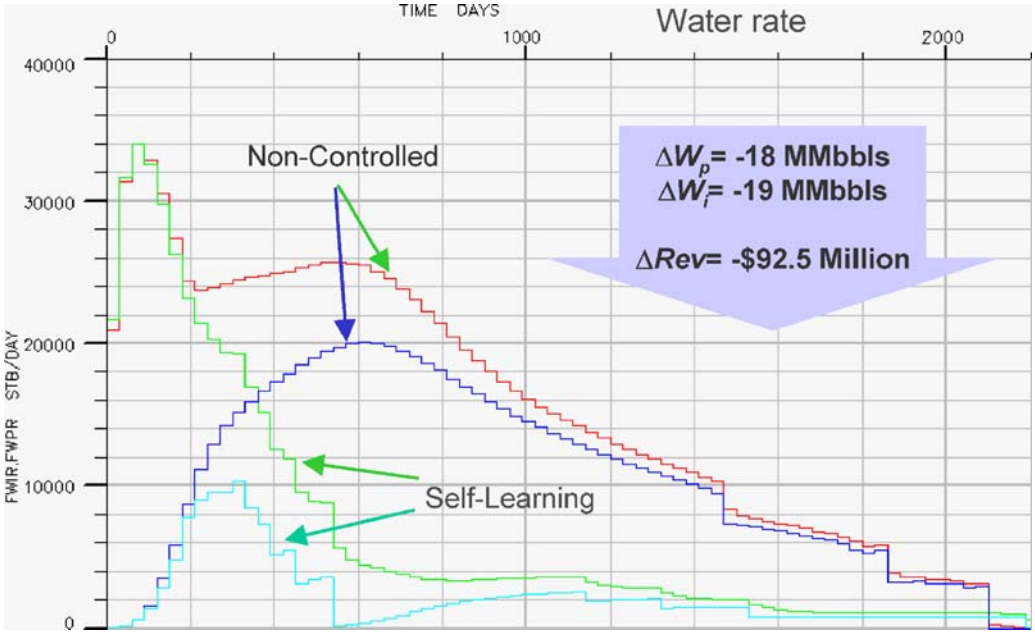

Figure 15. Water rate comparison (five-spot water drive problem).

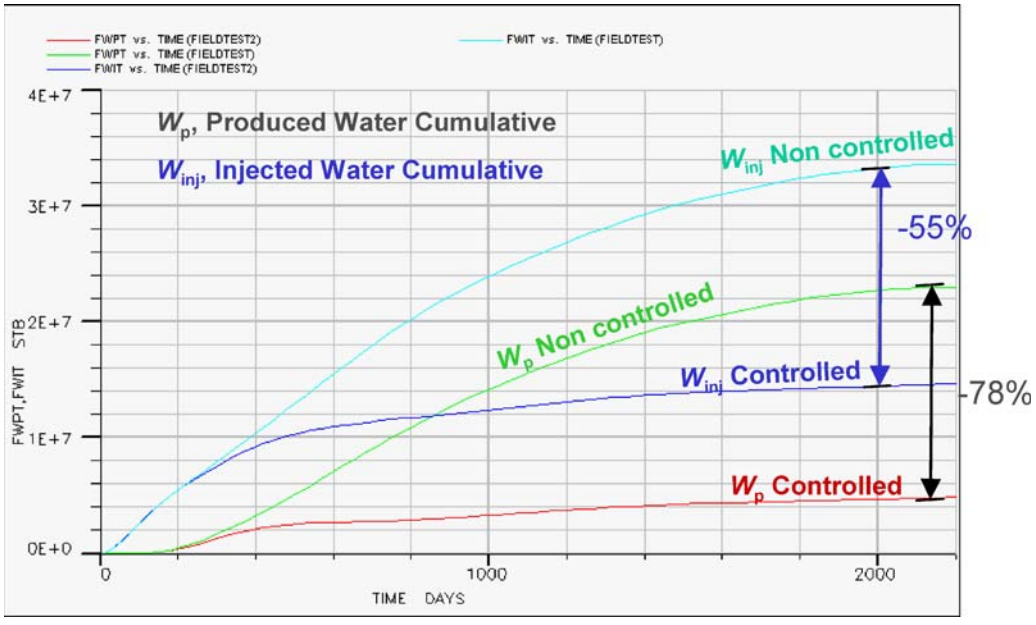

Figure 16. Water cumulative (five-spot water drive problem).

from flooded layers, automatic regulatory action will reduce the contribution from them (until shutoff), while meeting business objectives (water handling cost). Therefore, water rate was minimized for the self-learning case.

In the noncontrolled case, injected water is a response of the volume required to maintain constant pressure in the reservoir. The more water is produced, the more water needs to be injected to replace the produced volume (figure 15).

As a comparative result, the self-learning case (figure 16) was able to reduce cumulative water production by almost 80%, and reduce water injection by 55%. With an average price of 2.5$/bbl of water handling costs, either for compression or treatment, this rounds up to an additional project net present value of US$92.5 million, over the period of 2,200 days.

6. Suggestions for further directions

6.1. Continuous feedback adjustment

Tracking of setpoints of reservoir pressure, and production and injection rates (outputs) was effected by on-line adjustment of the flow settings (valve openings) of injectors and producers (inputs) in a feedback fashion. This was made possible by

having an adequate dynamic model that could predict the effect of inputs on controlled outputs. This model was continuously updated and used by the feedback controller (MPC), which was fed with optimal setpoints by an upper NPV optimization level. This approach is different from previous approaches found in literature, where optimization was attempted off-line in a fragmented fashion over a single time-scale.

6.2. *Disturbance rejection*

The MPC strategy was able to reject disturbances such as bottomhole pressure changes in adjacent completions, or pressure changes from the injector. A deeper analysis and disturbance rejection strategy may be developed as a consequence of these observations.

6.3. *Number of sensors and actuators*

The dependence of the ultimate outcome of the self-learning reservoir management strategy on the number and location of sensors and actuators was clearly demonstrated. By comparing various alternatives of increasing sensing and actuating capability, the current framework can guide further work to determine the optimal number and location of sensors and actuators required to implement an effective reservoir management strategy.

6.4. *Limited optimization ability*

Once the physical constraints were reached (minimum bottomhole and wellhead pressure), the controller's role was only to monitor the reservoir response, and no further inputs could be implemented. Thus, the system was not able to improve beyond this point. This creates an opportunity to interface the proposed strategy with an upper level of optimization that would select a different range of constraints or resizing of the system, for example, by making decisions to add new wells.

6.5. *Persistence of excitation*

No controller degradation was observed because identification was performed in closed loop. Model/process mismatch was acceptable for control purposes. Proper input excitation may be required for guaranteeing a well-conditioned information matrix during identification. If necessary, persistent excitation may be also embedded into the MPC algorithm, and the setpoint parameter would be changed by the allowable flow constraints. Remotely operated actuators (smart well completions and automated wellheads) will permit controlled continual excitation so that enough information is captured for identification.

6.6. *Fault-tolerant controller*

Further strategies may be added to the system to counter possible sensor or actuator faults. System redesign may also be suggested for enhanced fault tolerance, e.g., by hardware redundancy or virtual sensors.

6.7. *Extension to additional levels of the hierarchy in figure 1*

The approach presented in this paper, particularly the concepts of moving (receding) horizon and adaptation can also be used at higher levels of the operations hierarchy, reaching the capacity planning level.

7. Discussions and conclusions

In this work we have presented a methodology for self-learning reservoir management. The key features of that methodology are the following:

- A multilevel hierarchy of oilfield operations separates the real-time decision-making problem for an entire oilfield into a series of individual problems at different time-scales. The individual problems are computationally tractable by having relatively small dimensionality while they maintain relevance to the overall problem of optimizing an entire oilfield. This methodology has proven its value in the downstream industry and has the potential to greatly impact upstream operations.
- While modeling activity is commonplace in the upstream industry, what constitutes a useful model for a particular decision-making objective is not immediately obvious, yet it could have great impact on how real-time decisions are made. Model accuracy should be balanced with model simplicity and ease of use. In fact, it is estimates of those model features that are critical for a particular decision-making task that need to be optimized rather than an overall model quality index.
- Even though it may be applied at different time scales and different forms, feedback is indispensable for decision making. Models that are suitable for feedback-based decision making should be developed at all levels of the oilfield operations hierarchy.

Case studies were undertaken to demonstrate the proposed methodology. The studies were based on simulation data from a commercial simulator that was calibrated using historical production data. In one case study, application of the proposed methodology showed significant reduction of water injected (~55%) and produced (~80%), with simultaneous increase in overall oil recovery (~5%) over 2,200 days. The net result was that self-learning reservoir management strategy was able to

increase project profitability from 13% to 55%, corresponding to a net present value increase of US$ 92.5 million over the specified period. All shown case studies used homogeneous layer-cake reservoir models and exploitation scenarios of realistic complexity. Particular attention should be paid in future cases on more complex oilfied models. It is evident that with this paper, we have barely scratched the surface regarding what multilevel optimum decision making can bring to the upstream industry. Various possibilities for modeling, optimization, and control exist at all levels of the hierarchy shown in figure 1. This will be explored in our future work.

Nomenclature

a_0	Oil rate parametric coefficient (STB/day)
a_1, a_2, a_4	Oil rate parametric coefficient (STB/day/psi)
a_3	Oil rate parametric coefficient (STB/day/psi^2)
b_0	Water rate parametric coefficient (STB/day)
b_1, b_2, b_4	Water rate parametric coefficient (STB/day/psi)
b_3	Water rate parametric coefficient (STB/day/psi^2)
c_0	Gas rate parametric coefficient (MSCF/day) (not to be confused with oil compressibility, c_o, for oil)
c_1, c_2, c_4	Gas rate parametric coefficient (MSCF/day/psi)
c_3	Gas rate parametric coefficient (MSCF/day/psi^2)
d_0	Water injection parametric coefficient (STB/day)
d_1, d_2, d_4	Water injection parametric coefficient (STB/day/psi)
d_3, d_5	Water rate parametric coefficient (STB/day/psi^2)
C_F^k	Total fixed costs (overhead, leases, capital cost) at time interval k
C_{wp}	Cost of treatment and disposal of produced water per unit barrel [$/STB]
C_{wi}	Cost of treatment and compression of injected water per unit barrel [$/STB]
e_0	Pressure parametric coefficient (psi)
e_1, e_2, e_4	Pressure parametric coefficient (dimensionless)
e_3, e_5	Pressure parametric coefficient (l/psi)
ΔT_k	Size in days of the time interval
FIR	Finite impulse response
FOPR	Field oil production rate (STB)

FOPT	Field oil production cumulative (STB)
FPR	Field pressure (psia)
FWIR	Field water injection rate (STB/day)
FWIT	Field water injection cumulative (STB/day)
FWPR	Field water production rate (STB/day)
FWPT	Field water production cumulative (STB/day)
i	Annual discount factor
i_1, i_2	Injector 1, injector 2
J^*	Productivity index above bubble point (STB/day/psi)
I_{T}^k	Total capital investment on field assets (wells, surface facilities) at time interval k
k	Time interval number
MIMO	Multiple inputs and multiple outputs
MPC	Model predictive control
N	Number of measurements or intervals
n	Number of regression coefficients
Np	Cumulative produced oil (STB)
NPV	Net present value
nU	Number of inputs
nY	Number of outputs
p_1, p_2	Producer 1, producer 2
P_b	Bubble point pressure (psi)
P_o	Net selling revenues of oil [$/STB]
P_{g}	Net selling revenues of gas [$/SCF]
q_{wi}	Water injection rate (STB/day)
q^k	Flow rate at time k (STB/day)
$q_{p,sp}$	Setpoint of flow rate of phase p (STB/day)
q_{pi}	Flow rate of phase p, well i (STB/day)
q_p^k	Daily production of oil [STB/day], water [STB/day], and gas [SCF/day] at time interval k

q_{wi}^{k}	Daily injection of water [STB/day] at time interval k
r^{k}	Tax rate at time interval k
u_F	Future moves of the input variable vector
u_i	Input variable number i
We	Cumulative water injected (STB)
WOPR	Well oil production rate (STB/day)
Wp	Cumulative water production (STB)
y_i	Output variable number i

Appendix A: Parametric porous media modeling

Fluid rates

Oil, water, and gas rates are linearly related to a pressure integral function, which declines monotonically as time passes, or simply a linear relation between average reservoir pressure $\overline{P}$ and the well flowing pressure, p_{wf}, as,

$$q_o(t) \propto \frac{kh}{p_D}\int_{p_{wf}}^{\overline{P}} \frac{k_{ro}}{\mu_o \beta_o} \cong f_L\left(p_{wf}, \overline{P}\right), \tag{A1}$$

$$q_w(t) \propto \frac{kh}{p_D}\int_{p_{wf}}^{\overline{P}} \frac{k_{rw}}{\mu_w \beta_w} \cong f_L\left(p_{wf}, \overline{P}\right), \tag{A2}$$

$$q_g(t) \propto \frac{\beta_g (GOR - R_s) kh}{p_D}\int_{p_{wf}}^{\overline{P}} \frac{k_{ro}}{\mu_o \beta_o} \cong f_L\left(p_{wf}, \overline{P}\right), \tag{A3}$$

where k is the absolute permeability [md], h is the pay thickness [ft], k_{rp} is the relative permeability of phase p [fraction], β_p is the formation volume factor of phase p [rbbl/STB] or [rbbl/SCF], μ_p is viscosity of phase p [cp], GOR is the producing gas oil ratio, and $p_D = \ln(r_e/r_w)$ at steady state or $p_D = \ln(0.472 r_e/r_w)$ at pseudo-steady state conditions.Without loss of generality at any particular time, oil, water, and gas flows can be represented (in oilfield units) as,

$$q_o = \frac{k k_{ro} h \left(p_e - p_{wf}\right)_o}{141.2 \beta_o \mu_o [p_D + s],} \tag{A4}$$

$$q_w = \frac{k k_{rw} h \left(p_e - p_{wf}\right)_w}{141.2 \beta_w \mu_w [p_D + s].} \tag{A5}$$

For which flow functions can be simply modeled as

$$q_o^k = a_1 \cdot \overline{p}^k + a_2 \cdot p_{wf}^k, \tag{A6}$$

$$q_w^k = b_1 \cdot \overline{p}^k + b_2 \cdot p_{wf}^k, \tag{A7}$$

$$q_g^k = c_0 \cdot q_o^k, \tag{A8}$$

Recall that Vogel's backpressure and Fetkovich's equation for which flow *above* and *below* the bubble point pressure are

$$q_o = J^*(\overline{p} - p_b) + \frac{p_b J^*}{1.8}\left[1 - 0.2\left(\frac{p_{wf}}{p_b}\right) - 0.8\left(\frac{p_{wf}}{p_b}\right)^2\right], \tag{A9}$$

$$q_o(t) = J^*(\overline{p} - p_b) + \frac{J^*}{2p_b}\left[p_b^2 - p_{wf}^2\right]. \tag{A10}$$

Therefore, oil, water, and gas flows can be modeled as

$$q_o^k = a_0 + a_1 \cdot \overline{p}^k + a_2 \cdot p_{wf}^k + a_3 \cdot \left(p_{wf}^k\right)^2, \tag{A11}$$

$$q_w^k = b_0 + b_1 \cdot \overline{p}^k + b_2 \cdot p_{wf}^k + b_3 \cdot \left(p_{wf}^k\right)^2, \tag{A12}$$

$$q_g^k = c_0 + c_1 \cdot \overline{p}^k + c_2 \cdot p_{wf}^k + c_3 \cdot \left(p_{wf}^k\right)^2, \tag{A13}$$

and the values of $a_0, \ldots, a_3$, $b_0, \ldots, b_3$, $c_0, \ldots, c_3$ are the parameters to be fitted through regression. The equivalent matrix form is

$$\begin{bmatrix} q_o^k & q_w^k & q_g^k \end{bmatrix} = \begin{bmatrix} 1 & \overline{p}^k & p_{wf}^k & \left(p_{wf}^k\right)^2 \end{bmatrix} \begin{bmatrix} a_0 & b_0 & c_0 \\ a_1 & b_1 & c_1 \\ a_2 & b_2 & c_2 \\ a_3 & b_3 & c_3 \end{bmatrix}, \tag{A14}$$

Since measurements are taken continuously over time, a least-squares estimator can be used to approximate an optimum fitting parameter vector that best fits the experimental data; or any other technique such as partial least squares, neural networks, or subspace identification.

$$\begin{bmatrix} q_o^k & q_w^k & q_g^k \\ q_o^{k+1} & q_w^{k+1} & q_g^{k+1} \\ \vdots & \vdots & \vdots \\ q_o^N & q_w^N & q_g^N \end{bmatrix} = \begin{bmatrix} 1 & \overline{p}^k & p_{wf}^k & \left(p_{wf}^k\right)^2 \\ 1 & \overline{p}^{k+1} & p_{wf}^{k+1} & \left(p_{wf}^k\right)^2 \\ \vdots & \vdots & \vdots & \vdots \\ 1 & \overline{p}^N & p_{wf}^N & \left(p_{wf}^k\right)^2 \end{bmatrix} \begin{bmatrix} a_0 & b_0 & c_0 \\ a_1 & b_1 & c_1 \\ a_2 & b_2 & c_2 \\ a_3 & b_3 & c_3 \end{bmatrix} \quad \text{(A15)}$$

Reservoir pressure modeling

Recall a general material balance equation for oil or gas reservoirs, in which the time-dependent pressure function is related to mass-cumulative quantities

$$f[p(t)] = g\left(N_p, G_p, W_p, W_e\right), \quad \text{(A16)}$$

$$\overline{p} = a_0 + a_1 \int q_o + a_2 \int q_w + a_3 \int q_g + a_4 \int q_{wi}, \quad \text{(A17)}$$

$$\frac{d\overline{p}}{dt} = b_1 q_o + b_2 q_w + b_3 q_g + b_4 q_{wi}, \quad \text{(A18)}$$

and the values of $b_0, \ldots, b_5$ are the parameters to be fitted through regression. The equivalent matrix form of the time-dependent pressure function is

$$\left[(\overline{p})^k\right] = [\, b_0 \quad b_1 \quad b_2 \quad b_3 \quad b_4 \quad b_5 \,]\left[1 \quad \overline{p}^{k-1} \quad q_o^{k-1} \quad q_w^{k-1} \quad q_g^{k-1} \quad q_{wi}^{k-1}\right]^T, \quad \text{(A19)}$$

Combining the above with fluid rates models it is possible also to obtain:

$$\frac{1}{\Delta t}\left(\overline{p}^k - \overline{p}^{k-1}\right) \approx c_0 + c_1 \cdot \overline{p}^k + c_2 \cdot p_{wf1}^k + c_3 \cdot \left(p_{wf1}^k\right)^2 + c_4 \cdot p_{wf2}^k + c_5 \cdot \left(p_{wf2}^k\right)^2, \quad \text{(A20)}$$

Therefore, for $\Delta t = 1$, average reservoir pressure can be predicted as

$$(\overline{p})^k = e_0 + e_1 \cdot (\overline{p})^{k-1} + e_2 \cdot p_{wf1}^k + e_3 \cdot \left(p_{wf1}^k\right)^2 + e_4 \cdot p_{wf2}^k + e_5 \cdot \left(p_{wf2}^k\right)^2, \quad \text{(A21)}$$

and the values of $c_0, \ldots, c_3$ are the parameters to be fitted through regression. The equivalent matrix forms of the time-dependent pressure function is

$$\left[(\overline{p})^k\right] = [\, e_0 \quad e_1 \quad e_2 \quad e_3 \quad e_4 \quad e_5 \,]\left[1 \quad \overline{p}^k \quad p_{wf\,2}^k \quad \left(p_{wf1}^k\right)^2 \quad p_{wf2}^k \quad \left(p_{wf2}^k\right)^2\right]^T, \quad \text{(A22)}$$

Appendix B: Multivariate model predictive control formulation for reservoir management

Suppose that an oilfield process is described by some finite impulse response model as

$$\mathbf{Y}^k = \mathbf{H}\mathbf{U}^{k:k-N}, \tag{B1}$$

where

$$\mathbf{Y}^k = \begin{bmatrix} y_1^k & y_2^k & \cdots & y_q^k & \cdots & y_{nY}^k \end{bmatrix}; q = 1, 2, \ldots, nY, \tag{B2}$$

$$\mathbf{U}^k = \begin{bmatrix} \mathbf{u}_1^k & \mathbf{u}_2^k & \cdots & \mathbf{u}_i^k & \cdots & \mathbf{u}_{nU}^k \end{bmatrix}; i = 1, 2, \ldots, nU, \tag{B3}$$

$$\mathbf{u}_i^k = \begin{bmatrix} u_i^k & u_i^{k-1} & \cdots & u_i^{k-j} & \cdots & u_i^{k-N} \end{bmatrix}; j = 1, 2, \ldots, N, \tag{B4}$$

$$y_q^k = \sum_{i=1}^{nU} \sum_{j=1}^{\infty} \left(h_{ij}^q\right)\left(u_i^{k-j}\right) \cong \sum_{i=1}^{nU} \sum_{j=1}^{N} \left(h_{ij}^q\right)\left(u_i^{k-j}\right), \tag{B5}$$

At time k, the following objective function must be minimized

$$\min_{\Delta \mathbf{u}_i^{k+t-1}} \left\{ \sum_{t=1}^{p} \left(\widehat{\mathbf{Y}}^{k+t|k} - \mathbf{Y}^{SP}\right)^2 + R \sum_{i=1}^{nU} \sum_{t=1}^{m} \left(\Delta \mathbf{u}_i^{k+t-1|k}\right)^2 \right\}, \tag{B6}$$

Subject to the following constraints:

$$\mathbf{Y}_{\min} \leq \widehat{\mathbf{Y}}^{k+j|k} \leq \mathbf{Y}_{\max}; t = 1, \ldots, p, \tag{B7}$$

$$\mathbf{u}_{\min} \leq \mathbf{u}_{k+t-1|k} \leq \mathbf{u}_{\max}; t = 1, \ldots, m, \tag{B8}$$

$$\mathbf{u}_{k+v|k} = \mathbf{u}_{k+m-1|k}; v = m, \ldots, p-1. \tag{B9}$$

At time k, future process values can be estimated from finite impulse response model as

$$\widehat{y}_q^{k+t|k} = \sum_{i=1}^{nU} \sum_{j=1}^{p} \left(h_{ij}^q\right)\left(u_i^{k-j+t}\right) + \widehat{d}_q^{k|k}, \tag{B10}$$

where

$$\widehat{d}_q^{k|k} = y_q^k - \sum_{j=1}^{N} \left(h_{ij}^q\right)\left(u_i^{k-j+t}\right); t = 1, \ldots, m, \ldots, p. \tag{B11}$$

If we expand the future values of process output as

$$\mathbf{Y}_{\mathbf{F}}^{k} = \mathbf{H}\mathbf{U}^{k:k+p}, \tag{B12}$$

this could be rearranged as vector/matrix form,

$$\widehat{\mathbf{Y}}_F = \mathbf{H}_F\mathbf{U}_F + \mathbf{H}_P\mathbf{U}_P + \mathbf{Y}^k; \tag{B13}$$

The quadratic problem is set as to find the minimum of,

$$\left(\widehat{\mathbf{y}}_F - \mathbf{y}^{SP}\right)^T\left(\widehat{\mathbf{y}}_F - \mathbf{y}^{SP}\right) + \Delta\mathbf{u}_F^T\mathbf{R}\Delta\mathbf{u}_F =$$

$$\left(\mathbf{H}_F\mathbf{u}_F + \mathbf{H}_P\mathbf{u}_P + \mathbf{y}_k - \mathbf{y}^{SP}\right)^T\left(\mathbf{H}_F\mathbf{u}_F + \mathbf{H}_P\mathbf{u}_P + \mathbf{y}_k - \mathbf{y}^{SP}\right) + \left(\mathbf{D}\mathbf{u}_F + \mathbf{F}\mathbf{u}_P\right)^T\mathbf{R}\left(\mathbf{D}\mathbf{u}_F + \mathbf{F}\mathbf{u}_P\right) =$$

$$\mathbf{u}_F^T\left(\mathbf{H}_F^T\mathbf{H}_F + \mathbf{D}^T\mathbf{R}\mathbf{D}\right)\mathbf{u}_F + 2\mathbf{u}_F^T\left[\mathbf{H}_F^T\left(\mathbf{H}_P\mathbf{u}_P + \mathbf{y}_k - \mathbf{y}^{SP}\right) + \mathbf{D}^T\mathbf{R}\mathbf{F}\mathbf{u}_P\right] + \cdots \tag{B14}$$

and linear constraints

$$\mathbf{y}_{\min} \le \mathbf{H}_F\mathbf{u}_F + \mathbf{H}_P\mathbf{u}_P + \mathbf{Y}_k \le \mathbf{y}_{\max}, \tag{B15}$$

$$\mathbf{u}_{\min} \le \mathbf{u}_F \le \mathbf{u}_{\max} \tag{B16}$$

$$\mathbf{U}\mathbf{u}_F = 0, \tag{B17}$$

where

$$\mathbf{U} = \begin{bmatrix} & & -1 & 1 & & \\ & & & \ddots & \ddots & \\ & & & & -1 & 1 \end{bmatrix}_{(p-m)\times(m-1)\quad (p-m)\times(p-m+1)}. \tag{B18}$$

The above minimization is solved at each time k by finding the derivative of the quadratic problem as

$$\frac{d}{d\mathbf{u}}\left(\mathbf{u}^T\mathbf{A}\mathbf{u} + \mathbf{B}\mathbf{u} + \mathbf{C}\right) = 2\mathbf{A}\mathbf{u} + \mathbf{B} = 0 \Rightarrow \mathbf{u} = \tfrac{1}{2}\mathbf{A}^{-1}\mathbf{B}, \tag{B19}$$

Table 1C
Rock properties

Layer	ϕ	k_x	Depth (ft)	T_x	T_y	T_z	c_r (psi^{-1})
1	0.15	500	14,500	1	1	0	3×10^{-6}
2	0.15	200	14,600	1	1	0	3×10^{-6}
3	0.15	200	14,610	1	1	0	3×10^{-6}
4	0.15	200	14,630	1	1	0	3×10^{-6}
5	0.15	50	14,650	1	1	0	3×10^{-6}

Table 2C
Oil and gas densities under standard conditions

Fluid	ρ_{osc} (lb_m/ft^3)	Fluid	ρ_{osc} (lb_m/ft^3)
Oil	54.637	Gas	0.068432

Table 3C
Oil properties

Pressure (psia)	R_s (MSCF/STB)	B_o (bbl/STB)	μ_o (cp)	c_o (psi^{-1})
500	0.054	1.045	7,666	1.53×10^{-5}
714.286	0.055833	1.0474	7,366.34	1.53×10^{-5}
1,428.57	0.125625	1.08002	1,251.99	1.53×10^{-5}
2,142.86	0.215357	1.124	212.79	1.53×10^{-5}
2,857.14	0.335	1.18504	36.166	1.53×10^{-5}
3,571.43	0.5025	1.27335	6.1468	1.53×10^{-5}
4,285.71	0.75375	1.4094	1.04472	1.53×10^{-5}
4,642.86	0.933214	1.50811	0.430698	1.53×10^{-5}
5,000	1.1725	1.64093	0.177561	1.53×10^{-5}

where

$$\mathbf{A} = \left(\mathbf{H}_F^T \mathbf{H}_F + \mathbf{D}^T \mathbf{R} \mathbf{D}\right) \tag{B20}$$

$$\mathbf{B} = 2\left[\mathbf{H}_F^T \left(\mathbf{H}_P \mathbf{u}_P + \mathbf{y}_k - \mathbf{y}^{SP}\right) + \mathbf{D}^T \mathbf{R} \mathbf{F} \mathbf{u}_P\right]. \tag{B21}$$

Table 4C
Average physical and economic figures for El Furrial Field

Reservoir temperature	276 °F
Reservoir depth	14,000 ft
Average permeability	250 mD
Average porosity	13 %
Average crude gravity	27 API
Gas/Oil ratio	1,120 SCF/STB
Datum reservoir pressure	11,250 psia
Bubble point pressure	4,620 psia
Original oil in place	7,400 MMSTB
Target recovery factor	46 %
Activation index for adding new production	5,714 $/STB/day

The optimal value of u_k is sent to the process, the process is left to run until time $k + 1$, at which point the optimization problem is set up and solved again. The procedure is repeated indefinitely.

Appendix C: Data used for examples

A data sample from a particular reservoir (within El Furrial Field) is used in this paper. Tables 1C–4C average reservoir data have been previously correlated with history-matched production; these data values have been selected or adjusted to ease research's goals, without misrepresenting field reality.

Rock and fluid data for examples in this paper resemble reservoir characteristics from El Furrial Field, north of Monagas Basin, Venezuela. El Furrial is a giant reservoir with originally 6 billion STB of 21°API oil in place, currently producing about 500,000 STB/day from several independently hydraulic units.

Appendix D: Objective function

The *objective function*, e.g., for a waterflooding project, may be expressed as the finite sum of discounted cash flows during the project horizon

$$NPV = \sum_{k=1}^{N} \frac{\left[\left(q_o^k P_o + q_g^k P_g - q_{wp}^k C_{wp} - q_{wi}^k C_{wi}\right)\Delta T_k - I_T^k - C_F^k\right]\left(1 - r^k\right)}{(1+i)^{\frac{k\Delta T_k}{365}}} \tag{D1}$$

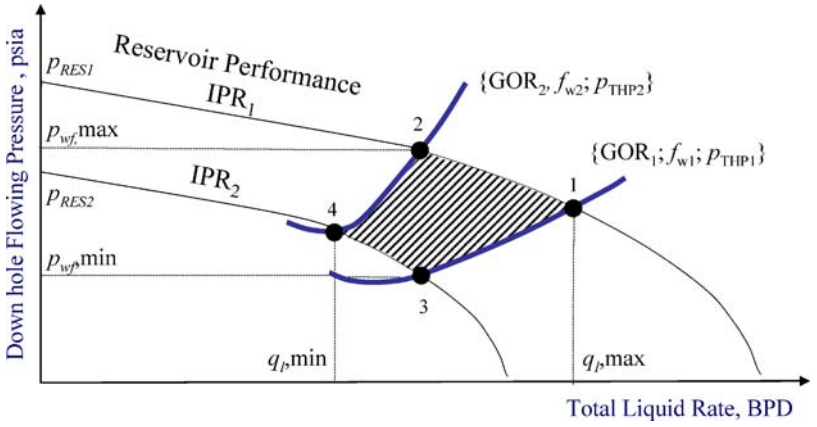

Figure 17. Well constraints vs. vertical lift performance.

where all the variables are defined in the nomenclature. Depending on the models used in equation (D1), the objective function may be a linear or nonlinear function of the constraints. Several methods may be used for different situations.

In practice, the way we achieve the optimal solution to equation (1) is that we assume a time model for q_o^k, q_g^k, q_{wi}^k, and q_{wp}^k, which allows us to find the cash flows in time, for certain assumptions in C_{wp}, C_{wi}, I_T^k, C_F^k, and i, and ultimately find a maximum (or minimum) value of equation (1) while honoring system constraints.

In the case of reservoir exploitation, these constraints are imposed by the reservoir, wells, surface equipment, cost, and schedule. For example, in finding the solution for optimizing the production rate of a well, the physical constraints are given by the reservoir productivity (IPR curves) and the tubing performance, as shown in figure 17. This figure shows the operating region of an oil well defined by two IPR curves and two tubing performance curves. The IPR curves (IPR_1, IPR_2) represent reservoir conditions at different static pressure (P_{RES1}, P_{RES2}) and well productivity indexes. Tubing performance is defined for two distinctive operating conditions of gas/oil ratio (GOR_1, GOR_2), water fraction (f_{w1}, f_{w2}) and tubing head pressure (p_{THP1}, p_{THP2}). Points 1–4 in figure 17 define the region of operability for this particular example.

$$\begin{cases} p_{wf}, \max \geqslant p_{wf} \geqslant p_{wf}, \min \\ q_l, \max \geqslant q_l \geqslant q_l, \min \end{cases} \tag{D2}$$

The shaded area in figure 17 denotes the region of feasible solutions.

References

[1] J. Murphy, Matching elegance and brawn: the challenges of smart well technology, Oil Gas J. (1999 April).
[2] L.A. Saputelli, S. Mochizuki, L. Hutchins, R. Cramer, M.B. Anderson, J.B. Mueller, A. Escorcia, A.L. Harms, C.D. Sisk, S. Pennebaker, J.T. Han, A. Brown, C.S. Kabir, R.D. Reese, A.R. Wood, G.J. Núñez, K. Landgren, C.J. McKie and C. Airlie, Promoting real-time optimization of hydrocarbon producing systems, SPE 83978 (2003).
[3] L. Saputelli, Real time reservoir simulation, SPE 51915 (1999).
[4] J.J. Arps, Estimation of decline curves, Trans. AIME 160 (1945) 228–247.
[5] J.V. Vogel, Inflow performance relationships for solution gas drive wells, JPT (1968, January) 83–92.
[6] J. Ternyik, H. Bilgesu, S. Mohaghegh and D. Rose, Virtual measurement in pipes, part 1: flowing bottom hole pressure under multi-phase flow and inclined wellbore conditions, SPE 30975 (1995).
[7] X. Zhu, Y.C. Soh and L. Xie, Design and analysis of discrete-time robust Kalman filters, Automatica 38 (2002) 1069–1077.
[8] F.E. Jansen and M.G. Kelkar, Application of wavelets to production data in describing inter-well relationships, SPE 38876 (1997).
[9] G. Renard, D. Dembele, J. Lessi and J.L. Mari, System identification approach applied to watercut analysis in waterflooded layered reservoirs, SPE 39606 (1998).

[10] S.J. Qin and T.A. Badgwell, A survey of industrial model predictive control technology, Control Eng. Pract. 11(7) (2003) 733–764.
[11] A.S. Cullick, D. Heath, K. Narayanan, J. April and J. Kelly, Optimizing multiple-field scheduling and production strategy with reduced risk, SPE 84239 (2003).
[12] V. Goel and I.E. Grossmann, A stochastic programming approach to planning of offshore gas field developments under uncertainty in reserves, Comput. Chem. Eng. 28(8) (2004) 1409–1429.
[13] P. Jacquard and C. Jain, Permeability distribution from field pressure data, Soc. Pet. Eng. J. (1965, December) 281–294.
[14] B. Yeten, L.J. Durlofsky and K. Aziz, Optimization of nonconventional well type, location and trajectory, SPE 77565 (2002).
[15] W. Ramirez, *Application of Optimal Control Theory to Enhanced Oil Recovery* (Elsevier, 1987).
[16] J.A. Holmes, T. Barkve and ∅. Lund, Application of a multi-segment well model to simulate flow in advanced wells, SPE 50646 (1998).
[17] F. Nyhavn, F. Vassenden and P. Singstad, Reservoir drainage with downhole permanent monitoring and control systems. Real-time integration of dynamic reservoir performance data and static reservoir model improves control decisions, SPE 62937 (2000).
[18] B. Yeten, L.J. Durlovsky and K. Aziz, Optimization of smart well control, SPE 79031 (2002).
[19] M. Litvak, L. Hutchins, R.C. Skinner, B. Darlow, R.C. Wood and L.J. Kuest, Prudhoe Bay E-field production optimization system based on integrated reservoir and facility simulation, SPE 77643 (2002).
[20] B. Sudaryanto, Optimization of displacement efficiency of oil recovery in porous media using optimal control theory, PhD Thesis, Southern California University, November, 1999.
[21] L. Ljung, *System Identification: Theory for the Users* (Prentice-Hall, Englewood Cliffs, NJ, 1987).
[22] L. Saputelli, H. Malki, J. Canelon and M. Nikolaou, A critical overview of artificial neural network applications in the context of continuous oil field optimization, SPE 77703 (2002).
[23] A.W. Moore, Cross-validation for detecting and preventing over fitting, www.cs.cmu.edu/∼awm/tutorials, 2001.
[24] H. Akaike, Information theory and the extension of the maximum likelihood principle, in *Second International Symposium on Information Theory*, eds. V.N. Petrov and F. Csaki, Akailseoniai-Kiudo, Budapest (1973), pp. 267–281.
[25] P. Albertos and A. Sala, *Multivariable Control Systems–An Engineering Approach* (Springer, 2004).
[26] H. Genceli and M. Nikolaou, New approach to constrained predictive control with simultaneous model identification, AIChE J. 42(10) (1996) 2857–2869.
[27] I.T. Jolliffe, *Principal Component Analysis* (Spriger Verlag, New York, USA, 1986).
[28] S. Wold, A. Ruhe, H. Wold and W. Dunn, The collinearity problem in linear regression: the partial least squares approach to generalized inverses, SIAM J. Sci. Stat. Comput. 5(3) (1984, September) 753–743.
[29] W.F. Ramirez and W. Liu, Interactive personal computer optimal control calculations for steamflooding, SPE 25523 (1992).
[30] B. Sudaryanto and Y.C. Yortsos, Optimization of displacements in porous media using rate control, SPE 71509 (2001).
[31] D.R. Brouwer and J.D. Jansen, Dynamic optimization of water flooding with smart wells using optimal control theory, SPE 78278 (2002).
[32] D.R. Brouwer, J.D. Jansen, S. van de Starr, C.P.J.W. van Kruijsdijk and C.W.J. Berentsen, Recovery increase through water flooding with smart well technology, SPE 68979 (2001).
[33] N.V. Queipo, J.V. Goicochea and S. Pintos, Surrogate modeling-based optimization of SAGD processes, SPE 69704 (2001).
[34] E.F. Camacho and C. Bordons, *Model Predictive Control* (Springer-Verlag, Berlin, 1999).
[35] J.B. Rawlings, Tutorial overview of model predictive control, IEEE Control Syst. Mag. 20(3) (2000, Jun) 38–52.

[36] M. Nikolaou, Model predictive controllers: a critical synthesis of theory and industrial needs, in *Advances in Chemical Engineering Series* (Academic Press, 2001).
[37] D.Q. Mayne, J.B. Rawlings, C.V. Rao and P.O.M. Scokaert, Constrained model predictive control: stability and optimality, Automatica 36(6) (2000) 789–814.
[38] M. Morari and E. Zafiriou, *Robust Process Control* (Prentice-Hall, 1989).
[39] Schlumberger, *Eclipse Reservoir Simulator Reference Manual* (UK, 2001).